

To see the latest GeoStudio learning content, visit <u>Seequent Learning Centre</u> and search the catalogue for "GeoStudio".

Introduction

Closed-form solutions for the bearing capacity of shallow footings are often used to verify finite element elastic-plastic formulations, since the bearing capacity equations are largely based on the soil being perfectly plastic. The objective here is to compare the ultimate bearing pressure from closed-form solutions with the results from a SIGMA/W analysis.

Background

The ultimate bearing pressure of a continuous strip footing at the ground surface is:

$$q_{ult} = N_c S_u + \frac{1}{2} \gamma B N_{\gamma} \label{eq:qult}$$
 Equation 1

where S_u is the undrained strength, q is related to overburden pressures at the footing level, B is the footing width and $^\gamma$ is the unit weight of the soil. Bearing capacity factors N_c , N_q , and $^{N_\gamma}$ will be taken from two different sets presented by Bowles, J.E. (1988) p. 116 & p. 118). Scanned copies of the tables are presented below for convenient reference (Table 1 and Table 2).

A quick glance at the two sets of bearing capacity factors reveals that they give quite different ultimate bearing pressures. This is common amongst the bearing capacity parameters presented by various authors, as discussed by Bowles, J.E. (1988).

Table 1. Bearing capacity factors from Table 4-1 in Bowles, J.E. (1988).

Table 4-1. Bearing-capacity factors for use in Eqs. (4-1) to (4-3) for general-shear conditions N_c , N_q , N_γ and local-shear conditions N_c , N_q' , N_γ'

φ	N_c	N_q	N_{γ}	N_c'	N_q'	N_{γ}'
0	5.7	1.0	0.0	5.7	1.0	0.0
5	7.3	1.6	0.5	6.7	1.4	0.2
10	9.6	2.7	1.2	8.0	1.9	0.5
15	12.9	4.4	2.5	9.7	2.7	0.9
20	17.7	7.4	5.0	11.8	3.9	1.7
25	25.1	12.7	9.7	14.8	5.6	3.2
30	37.2	22.5	19.7 -	19.0	8.3	5.7
34	52.6	36.5	35.0	23.7	11.7	9.0
35	57.8	41.4	42.4	25.2	12.6	10.1
40	95.7	81.3	100.4	34.9	20.5	18.8
45	172.3	173.3	297.5	51.2	35.1	37.7
48	258.3	287.9	780.1	66.8	50.5	60.4
50	347.5	415.1	1,153.2	81.3	65.6	87.1



Table 2. Bearing capacity factors from Table 4-2 in Bowles, J.E. (1988).

Table 4-2. Bearing-capacity factors N_c , N_q , and N_γ and ϕ -dependent terms for use in the shape factor s_c and d_q of Eq. (4-6)

φ	N_c	N_q	N_{γ}	N_q/N_γ	$2 \tan \phi (1 - \sin \phi)^2$
0	5.14	1.0	0.0	0.19	0.000
5	6.49	1.6	0.1	0.24	0.146
10	8.34	2.5	0.4	0.30	0.241
15	10.98	3.9	1.2	0.36	0.294
20	14.83	6.4	2.9	0.43	0.315
25	20.72	10.7	6.8 -	0.51	0.311
26	22.25	11.9	7.9	0.53	0.308
28	25.80	14.7	10.9	0.57	0.299
30	30.14	18.4	15.1	0.61	0.289
32	35.49	23.2	20.8	0.65	0.276
34	42.16	29.4	28.8	0.70	0.262
36	50.59	37.8	40.1	0.75	0.247
38	61.35	48.9	56.2	0.80	0.231
40	75.31	64.2	79.5	0.85	0.214
45	133.87	134.9	200.8	1.01	0.172
50	266.88	319.1	563.6	1.20	0.130

Numerical Simulation

Figure 1 presents the model domain and finite element mesh used in this example. There are three analyses in the Analysis Tree (Figure 2). The first analysis is an *in situ*, gravity activation analysis that acts as the Parent to the frictional and undrained analyses. Both the frictional and undrained analyses use the Load/Deformation analysis type.

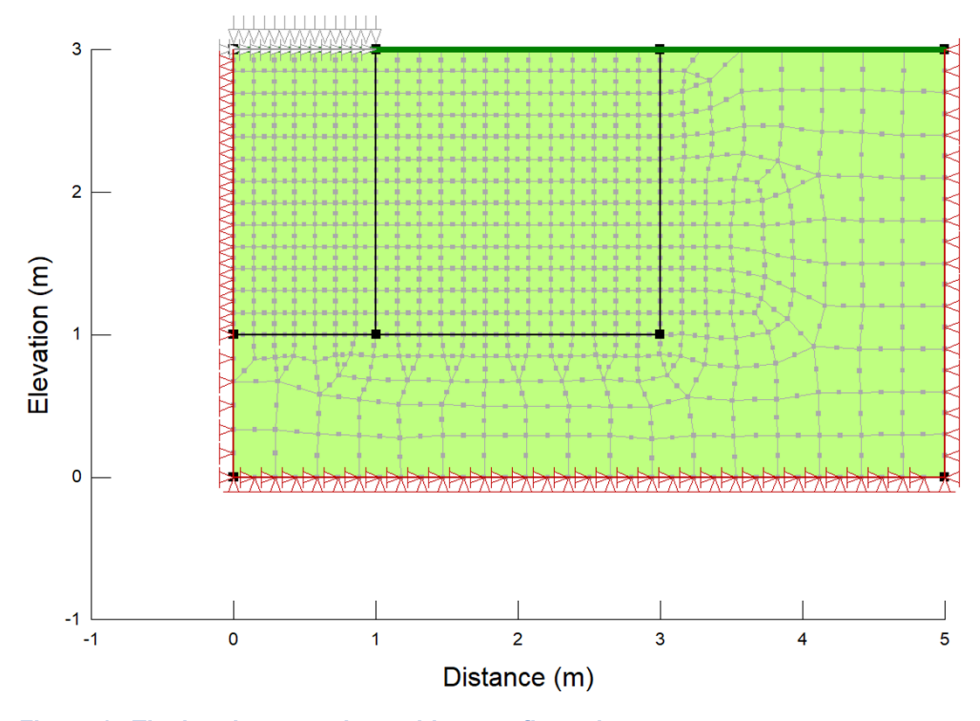


Figure 1. The bearing capacity problem configuration.





Figure 2. Analysis Tree for the Project.

The soil is assumed to have a unit weight of 20 kN/m³, elastic modulus of 100,000 kPa, and Poisson's ratio of 0.334. The footing width is 2 m. The bearing capacity analysis for the frictional case is completed using a friction angle of 30 degrees and the Mohr-Coulomb material model. The bearing capacity analysis for the undrained case is completed using an undrained strength of 100 kPa and the Tresca material model.

The mesh consists of 8-noded quadrilateral elements with 4 point integration. The depth is 2x the footing width and the length is 4x the footing width. The left side is the centre-line symmetric axis, and so only half of the problem is required for the numerical analysis. The actual footing width is 2 m (1 m in the finite element analysis).

The footing loads are applied as a displacement boundary condition function (Figure 3). The footing is being pushed into the ground at a constant rate, and SIGMA/W computes the equivalent forces required for the specified displacement. The bearing capacity analyses for the frictional and undrained cases are being completed in 32 load steps with a total vertical displacement of -0.02 m.

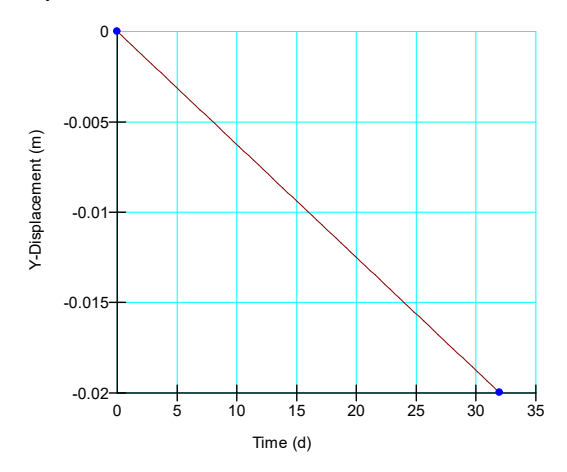


Figure 3. Vertical displacement function for the footing load.

Results and Discussion

Figure 4 presents yield zone and displacement pattern for the frictional case. The yield zone develops with a log-spiral form, which is in agreement with theoretical predictions. The greatest displacements are confined to the yield zone. Figure 5 shows the load-deformation response at the base of the footing and indicates an ultimate bearing capacity of about 320 kPa. The closed-form bearing capacity equation is given by:

$$q_{ult} = \frac{1}{2} \gamma B N_{\gamma} = \frac{1}{2} (20)(2) N_{\gamma}$$
 Equation 2



The bearing capacity factor N_{γ} ranges between 15.1 or 19.7 according to the above tables, which corresponds to an ultimate bearing capacity ranges between 302 kPa to 394 kPa.

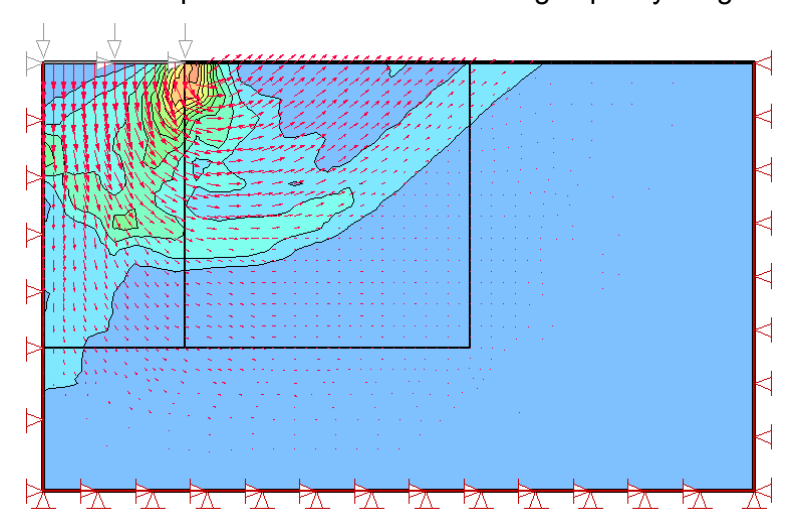


Figure 4. Log-spiral yield zone and displacement pattern.

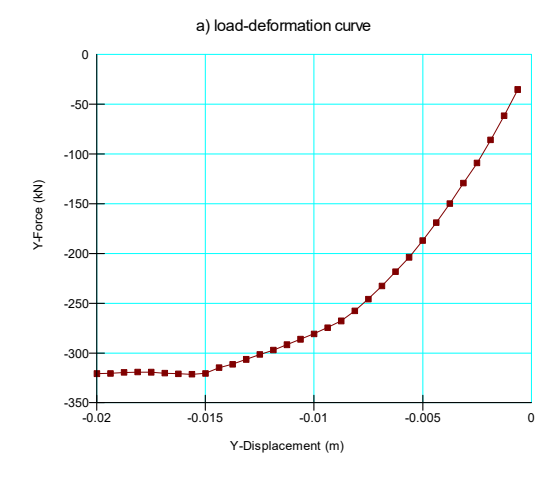


Figure 5. Load-deformation curve for the frictional soil case.

Figure 6 presents the yield zone and displacement pattern for the undrained case. The displacement pattern is circular and the yield zones form triangular wedges beneath the footing. Figure 7 shows the load-deformation response at the base of the footing and indicates an ultimate bearing capacity of about 550 kPa. The closed-form bearing capacity equation is given by:

$$q_{ult} = N_c S_u$$
 Equation 3

The bearing capacity factors for this case are 5.14 or 5.70 according to the above tables. The ultimate bearing capacity, therefore, ranges between 514 and 570 kPa.



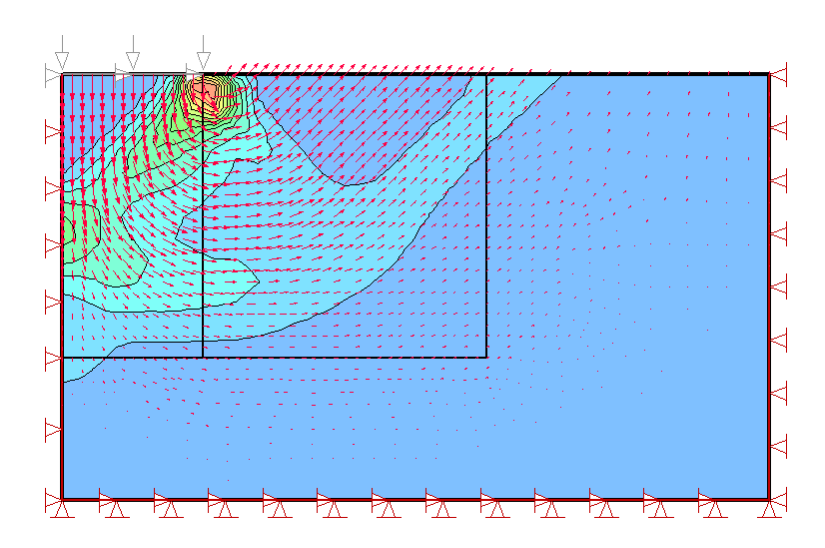


Figure 6. Circular displacement pattern with 'wedge' failures beneath the footing.

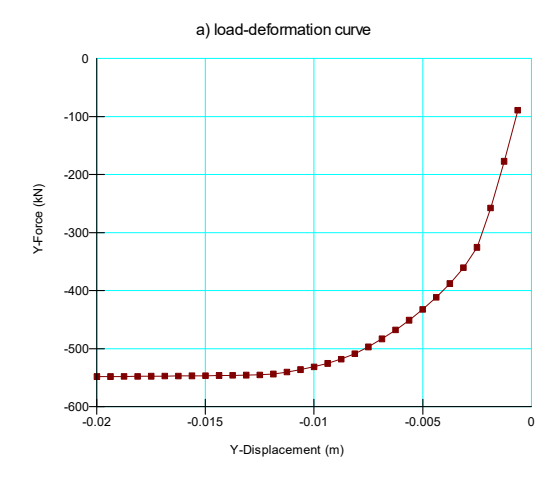


Figure 7. Load-deformation curve for the undrained case.

Summary and Conclusions

Bearing capacity problems can be particularly difficult to simulate for a number of reasons. The elements beneath the corner of the footing are pulled into tension, and can undergo large deformations. The finite element matrices can become ill-conditioned, and a solution could become difficult. The more pertinent issue, however, is the continued redistribution of the unbalanced forces once the yield zone is fully developed (i.e. global failure is occurring). The convergence requirements (i.e. number of iterations) can be demanding, resulting in long computational times and 'drift' or undulations (e.g. Figure 5) of the load-deformation curves. Stated another way, it is numerically difficult to follow the failure path because a global failure has occurred.

References

Bowles, J.E. 1988. *Foundation Analysis and Design*, 4th Edition. McGraw-Hill Inc. New York. p. 116-124.

